BOOSTER SYNCHROTRON FOR SIRIUS LIGHT SOURCE

F. H. Sa*, L. Liu, A. R. D. Rodrigues, LNLS, Campinas-SP, Brazil

Abstract

A full energy 3 GeV booster for the new Brazilian Synchrotron Light Laboratory (LNLS) third generation light source, SIRIUS, is proposed. The 144 m circumference magnetic lattice consists of two super-periods of FODO cells with defocusing dipoles and focusing quadrupoles. The optics provides a low emittance beam of 38 nm.rad at 3 GeV, high horizontal betatron and zero dispersion functions at straight sections. The top-up operation requires a cycling energy ramp from 150 MeV to 3 GeV with repetition rate of 1 Hz.

INTRODUCTION

The main goals of the design of the Booster lattice were:

- low emittance optics, for a clean top-up injection;
- small circumference, to reduce costs and space and ease maintenance, but large enough to accommodate the LINAC inside it;
- simple injection and extraction systems;
- small magnets with reduced aperture, to facilitate construction and characterization.

Fig. 1 shows SIRIUS injection system layout and Table 1 presents the general parameters of the Booster. The proposed design is a 2-fold symmetric lattice composed of 20 regular FODO cells, four missing dipole cells, two long straight sections of 5.5 m, one for extraction and other for the RF cavities, and four short ones of 2.8 m, for injection and the extraction kicker.

A total of 48 dipole magnets of 1.2 m and magnetic field of 1.09 T are used. The 32 quadrupoles are divided in four families, with maximum field gradient of 24.0 T/m and length of 0.3 m. The repetition rate value was chosen based on the storage ring filling time and power supply requirements.

Table 1: General Parameters of the Booster Design

Energy	E [GeV]	0.15 | 3.0
Circumference	C [m]	143.900
Revolution Time	T [ns]	480
Injected Emittance	ϵ [nm.rad]	170
Injected Energy Spread	σ_E/E [%]	0.5
Repetition rate	[Hz]	1

LATTICE

Table 2 presents the Booster lattice main parameters and Fig. 2 shows the optical functions for one super-period.

* fernando.sa@lnls.br

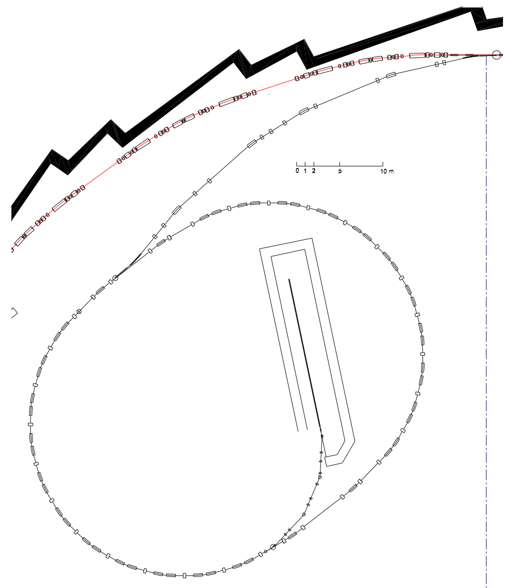

Figure 1: Layout of the injection system for SIRIUS storage ring.

Each FODO cell consists of two defocusing dipoles, split in half to achieve the small magnet requirement, and focusing quadrupoles.

Table 2: Booster Lattice Parameters at 0.15 and 3 GeV

Energy loss per turn	U_0 [KeV]	0.0049	782
Dipole Field	B_0 [T]	0.055	1.09
Natural Emittance	ϵ_0 [nm.rad]	0.09	37
Damped energy spread	σ_E/E [%]	0.0065	0.13
Horizontal damping time	τ_x [ms]	13700	1.7
Vertical damping time	τ_z [ms]	37400	3.7
Longitudinal damping time	τ_E [ms]	34700	4.3
Working point	ν_x/ν_y	7.43/3.24	
Natural chromaticities	ξ_x/ξ_y	-10.3/-5.8	
Momentum compaction	α_c	12.9×10^{-3}	

To correct chromaticities to zero in both transverse planes, two sextupoles families are installed, totalizing eight elements along the ring. These non-linear components limit the dynamic aperture to ±15 mm in the horizontal and ±10 mm in the vertical plane in the center of the long straight section, as shows the frequency map in Fig. 3. This aperture is about the same size of physical limitation and is sufficient for the Booster purposes.

The physical apertures were defined to allow a beam stay clear of four times the rms beam size at injection plus the maximum value of the closed orbit distortion obtained after correction, for the set of errors tested, and, for the hor-

ISBN 978-3-95450-115-1

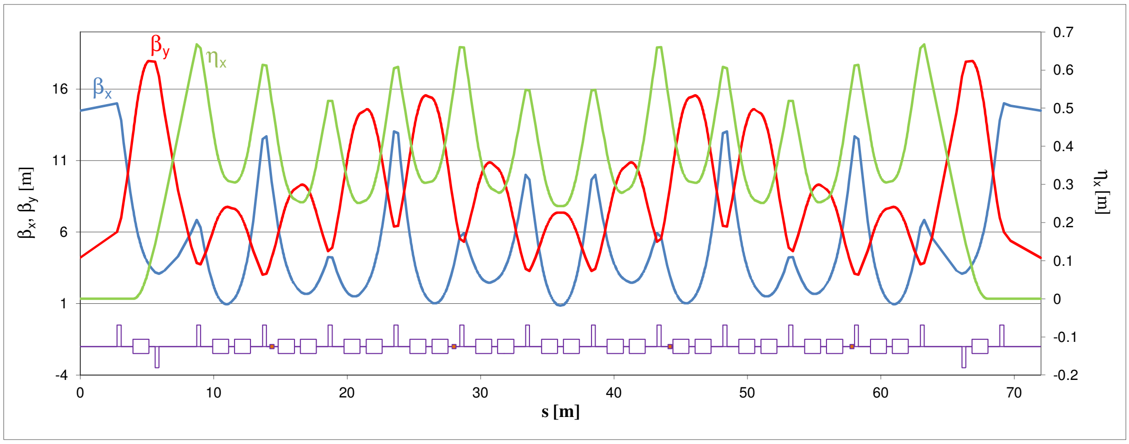

Figure 2: Optical functions of one super-period of the Booster.

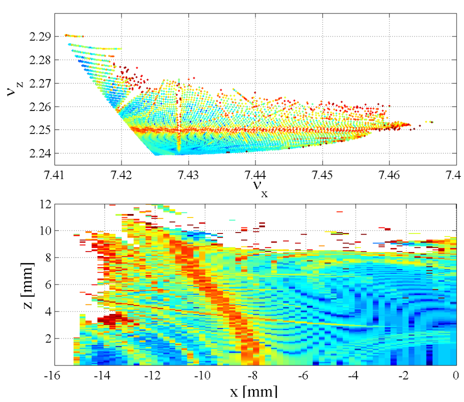

Figure 3: Frequency map of the Booster obtained from tracking of two thousand turns. Scale goes from blue, equivalent to change of 10^{-12} in tune, to red, 10^{-2}.

izontal plane, we also took into account 1 mm of residual oscillation after the injection and an oscillation due to energy variations of the beam coming from LINAC. Thus, at straight sections the chamber will be circular with internal diameter of 35 mm and at the dipoles it will be elliptic with internal axis of 40×19 mm^2.

The four quadrupole families allow a large tune range for the machine and independent control of the dispersion in the straight sections, which is important to escape from resonances and change the operational mode for better global characteristics, such as emittance, energy spread or momentum compaction, if necessary.

INJECTION AND EXTRACTION

The injection will take place at a short straight section, which is dispersive. A 15° septum will deliver the beam 24 mm away from Booster axis. One meter downstream, the beam will cross the axis and a 25 mrad fast kicker will set its angle to zero.

The extraction system consists of one fast kicker and two septa. The 2.3 mrad fast kicker, located in a short straight section, kicks the beam to the 4.5° thin septum, in the long straight section, at 16 mm from the axis. The thin septum will conduct the beam to a 8.5° thick septum, which will extract it from the ring.

All septa blades thickness will be 4 mm, to generate low leak field and cause a peak closed orbit distortion lower than 1 mm. Also, in both systems the beam center will have a clearance of more than three-sigma from the septum blade. Fig. 4 shows the injection and extraction schemes for the Booster.

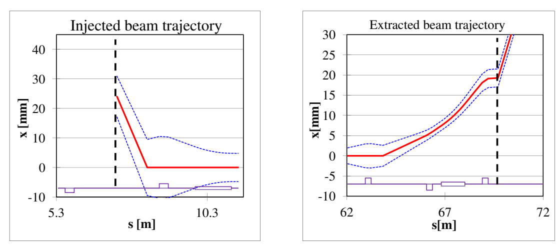

Figure 4: Injected and extracted beam trajectories. In red, the beam center and in blue ±3-beam size at injection/extraction. The point where beam center crosses the axis indicate the positions of the kicker and the vertical line the end/beginning of the thin septa.

RF SYSTEM

Table 3 shows the main parameters related to the RF system. At low energy, the RF voltage must provide an energy acceptance which capture the bunch train coming from the LINAC and, at the extraction energy, it must provide a quantum lifetime larger than 10 seconds. Due to the large damped energy spread and momentum compaction of the Booster at 3 GeV, this value is quite demanding.

Two possibilities for the RF cavities are under study: two PETRA 5-cell cavities or one PETRA 7-cell cavity. The total power required for both options are 37 and 83 kW respectively. The power source will be based on solid state RF amplifier technology.

Table 3: RF Parameters at 150 MeV and 3 GeV

Harmonic number	H	240 ($2^4 \cdot 3 \cdot 5$)	
RF frequency	f_{RF} [MHz]	500	
Multi-bunch current	I [mA]	<10	
RF Voltage	V [MV]	0.2	1.75
Overvoltage	Q	∞	2.24
Synchrotron frequency	f_s [kHz]	53.4	33.4
Synchronous phase	ϕ_s [°]	180	153.5
Natural Bunch length	σ_L [mm]	15.2	24
Energy acceptance	[%]	1.65	0.69
Quantum lifetime	[s]	∞	209

CLOSED ORBIT CORRECTION

The closed orbit correction system will have 28 BPMs, 28 horizontal and 24 vertical correctors. The system was tested with random alignment and excitation errors applied to the magnets of the machine. The errors have gaussian distribution with a cut-off in two-sigma. Table 4 presents the standard deviations of the errors and Fig. 5 shows the closed orbit distortion before and after correction for 100 random machines. The maximum corrector strength was limited to 1 mrad.

Table 4: Standard Deviations of the Errors Used to Test the Orbit Correction System

Error Type	Dipoles	Quadrupoles	Sextupoles
ΔX [mm]	0.100	0.100	0.100
ΔY [mm]	0.100	0.100	0.100
Excitation [%]	0.1(0.2)	0.2	0.2
Roll [mrad]	0.5	0.5	0.5
Yaw [mrad]	0.5	0.5	0.5
Pitch [mrad]	0.5	0.5	0.5

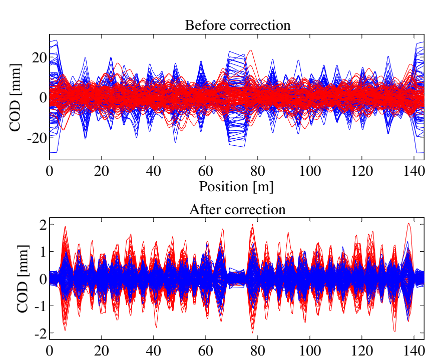

Figure 5: Closed orbit distortion for one hundred machines with random errors. Red lines represent the vertical and blue lines, the horizontal plane.

ENERGY RAMP EFFECTS

The energy ramp will be sinusoidal and the RF voltage ramp will be linear. This define how parameters like emittance and energy spread will evolve during the ramp process. Both will shrink from the injected value to final equilibrium values, first due to the acceleration itself and then due to radiation emission. Fig. 6 show the ramping behavior of the quantities discussed above.

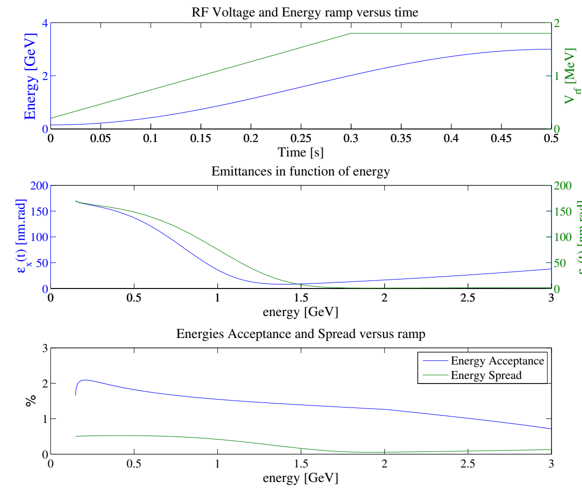

Figure 6: Evolution of emittances and energy spread in function of energy ramp of the Booster.

On the other hand, the variation of the magnetic field in the magnets vacuum chamber, mainly dipoles, will induce eddy current and consequently a sextupolar gradient in those regions. Fig. 7 presents the chromaticities changes expected for a elliptic stainless steel vaccum chamber 1 mm thick. The values achieved are easily corrected with the two lattice sextupole families.

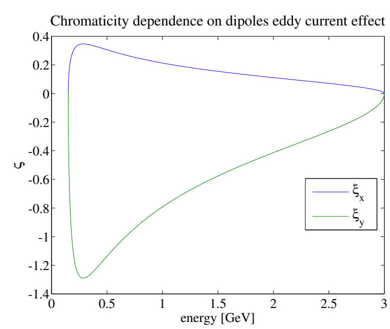

Figure 7: Chromaticities induced by eddy currents on the dipoles vacuum chambers due to the ramping process.

CONCLUSIONS

The Booster design proposed in this work achieves the main objectives required, such as low emittance, small magnets and small circumference. However, the RF system requires a very demanding voltage, which will request a detailed analysis of the possible choices for the RF cavities in order for the Booster to have a system that conciliates low costs and high quality.

ISBN 978-3-95450-115-1